Journal of the Iranian Chemical Society (2022) 19:2883–2890
https://doi.org/10.1007/s13738-022-02502-1

ORIGINAL PAPER

Adsorption and removal mechanism of Pb(II) by oxidized multi-walled carbon nanotubes

Qiuping Fu[1] · Jie Lou[1] · Denghong Shi[1] · Shaoqi Zhou[2] · Jing Hu[2] · Qi Wang[1] · Weijiang Huang[1] · Kui Wang[1] · Wei Yan[1]

Received: 8 October 2021 / Accepted: 7 January 2022 / Published online: 10 February 2022

Abstract

Multi-walled carbon nanotubes (MWCNTs) were treated by reflux oxidation in a mixture (HNO_3 and H_2SO_4), hydroxyl (–OH) and carboxyl (–COOH) functional groups were introduced on the surface of MWCNTs to obtain the Oxidized-MWCNTs (OMWCNTs). OMWCNTs were used as adsorbent to removal of Pb(II) from wastewater. The effects of contact time, initial concentration of Pb(II), OMWCNTs dosage, pH and coexisting ions (K^+, Na^+, Ca^{2+}, Mg^{2+}) on the adsorption and removal of Pb(II) by OMWCNTs were systematically studied. The adsorption of Pb(II) by OMWCNTs could reach equilibrium in 10 min. The pH > 5 is conductive to the adsorption of Pb(II) by OMWCNTs. The coexisting ions (K^+, Na^+, Ca^{2+}, Mg^{2+}) had almost no effect on the adsorption of Pb(II) by OMWCNTs. The results showed that the isothermal data fit the Freundlich and Langmuir isotherm models. The maximum adsorption capacity was 558.66 mg/g for Pb(II) from Langmuir isotherm. The pseudo-second-order kinetic model could well describe the adsorption process of Pb(II).

Keywords MWCNTs · Oxidation modification · Heavy metal ions · Pb(II) · Adsorption

Introduction

With the rapid development of economy and the acceleration of industrialization process, battery manufacture, mining, steel, electroplating, leather, paper making, petrochemical, pesticide and other industries have developed rapidly, and a large amount of wastewater containing heavy metal ions is produced [1–3]. Heavy metal ions could pose a serious threat to ecological environment and human health. Pb(II) is a typical heavy metal ion. Pb(II) excessive entry into human body can lead to health problems such as dysfunction of kidney, reproductive system, liver, central nervous system, and even various cancers [4, 5]. Therefore, it is of great significance to prevent Pb(II)—containing wastewater from being discharged into the environment.

The treatment methods of wastewater mainly include chemical precipitation, electrolysis, ion exchange, membrane separation and adsorption [6–9]. Adsorption method has been widely used because of its simplicity and convenience [10–12]. But the key of adsorption method is to choose proper adsorbent. As we all know, carbon nanotubes (CNTs) are porous materials with unique pore cavity structure, high specific surface area and strong adsorption performance [13]. CNTs have no destructive effect on the water environment. On the contrary, it has a good migration and transformation effect on the toxic organic compounds that may exist in water [14, 15]. The studies show that CNTs containing carboxyl and hydroxyl groups with good adsorption effect on heavy metals could obtain by oxidation treatment of CNTs [16, 17].

In this paper, MWCNTs with poor dispersion in water were taken as the research object. MWCNTs were oxidized by mixed acid (volume ratio of nitric acid to sulfuric acid is 3:1) to improve their dispersion in aqueous solution, and then obtained OMWCNTs. The adsorption capacity of Pb(II) on MWCNTs before and after oxidation were compared experimentally. The influences of contact time, dosage of OMWCNTs, pH and co-existing ions (Na^+, K^+, Ca^{2+}, Mg^{2+}) on the adsorption of Pb(II) were systematically studied. The adsorption mechanism of Pb(II) by OMWCNTs

✉ Qiuping Fu
taochao5@163.com

✉ Shaoqi Zhou
2975742087@qq.com

[1] College of Chemistry and Materials Engineering, Guiyang University, Guiyang 550005, China

[2] College of Resource and Environmental Engineering, Guizhou University, Guiyang 550003, China

was discussed from the aspects of isothermal adsorption, adsorption kinetics and XPS characterization.

Experiment

Materials

Multi-walled carbon nanotubes (MWCNTs) (purity > 90 wt%, outer diameters of 8 ~ 15 nm, length of 30 ~ 50 μm) were purchased from Aladdin Chemical Reagent Co., Ltd. Nitric acid (HNO_3), sodium hydroxide (NaOH) were analytical pure and purchased from Sinopharm Chemical Reagent Co., Ltd. Both sulfuric acid (H_2SO_4), potassium nitrate (KNO_3), calcium nitrate ($Ca(NO_3)_2$) were all analytical pure and purchased from Chengdu Jinshan Chemical Reagent Co., Ltd. Hydrochloric acid (HCl) was analytical pure and purchased from Taicang Lutest Reagent Co., Ltd. Sodium nitrate ($NaNO_3$), magnesium nitrate ($Mg(NO_3)_2$) were all analytical pure and purchased from Tianjin Kemiou Chemical Reagent Co., Ltd. Lead acetate ($PbC_4H_6O_4{\cdot}3H_2O$) was analytical pure and purchased from Aladdin Chemical Reagent Co., Ltd. All reagents employed in this study were used as received.

Preparation of OMWCNTs

OMWCNTs were obtained by reflux reaction of 500 mg MWCNTs and 100 mL mixed acid for 6 h at 100 °C. The suspension were cooled to room temperature and then cleaned with ultra-pure water until the pH of the suspension reached about 7. The OMWCNTs were obtained after drying in oven at 60 °C.

Adsorption experiments

Adsorption experiments were carried out to study the influence of contacting time, absorbent dosage, pH value and coexisting ions on the adsorption and removal of Pb(II) by OMWCNTs at 30 °C. For studying the influence of contacting time, 10 mg OMWCNTs was added in 25 mL different initial Pb(II) concentrations (10–100 mg/L) shocking for 5 ~ 120 min. For studying the influence of absorbent dosage, OMWCNTs (dosage of 10, 15, 20, 25, 30, and 35 mg) was added in 25 mL 80 mg/L Pb(II) containing wastewater shocking for 30 min. For studying the pH value, 10 mg OMWCNTs was added in 25 mL 80 mg/L Pb(II) containing wastewater with different initial pH value (2–7) adjusted by using HCl/NaOH shocking for 30 min. For studying the coexisting ions, 10 mg OMWCNTs was added in 25 mL 80 mg/L Pb(II) containing wastewater with different concentration of the coexisting ions shocking for 30 min. Then, Pb(II) concentration of the filtrate was measured by atomic absorption spectrophotometer.

Characterization

X-ray diffraction (XRD) patterns of MWCNTs and OMWCNTs were characterized by the Rigaku Ultima-IV X-ray diffractometer (Rigaku, Japan). Fourier transform infrared (FT-IR) spectra of OMWCNTs was detected by FT-IR spectrometer (Shimadzu, Japan). The morphology of OMWCNTs was observed by the scanning electron microscopy (SEM). X-ray photoelectron spectroscopy (XPS) of OMWCNTs was measured by the Thermo Scientific K-alpha spectrometer. Pb(II) concentration was measured by using a AA-7000 atomic absorption spectrophotometer.

Results and discussion

Characterization of the adsorbents

Figure 1 shows the XRD patterns of MWCNTs and OMWCNTs. It can be seen from the figure that the diffraction peaks of MWCNTs and OMWCNTs are basically the same, and their diffraction peaks ($2\theta = 25.9, 42.8$) are corresponded of the graphite phase (JCPDS No. 41-1487) [18]. It indicates that the structure of MWCNTs does not change significantly after oxidation treatment. In addition, the diffraction peaks of MWCNTs and OMWCNTs are sharp, indicating that they have high crystallinity.

Figure 2 shows the FT-IR spectrum of OMWCNTs. It can be seen from the figure that there are many peaks of containing oxygen groups in FT-IR spectrum. The peaks near 3322 and 2921 cm^{-1} belong to the bands of –OH

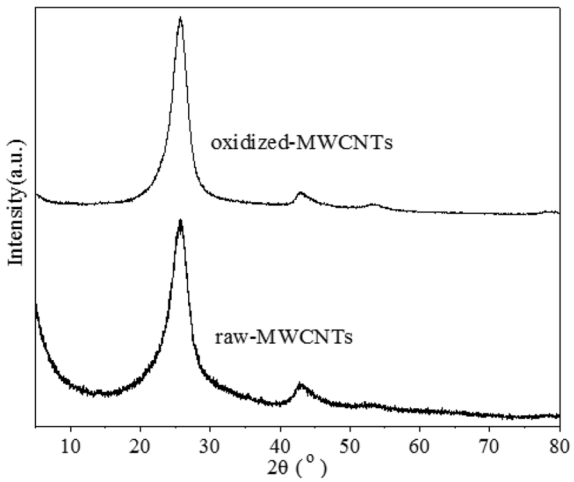

Fig. 1 XRD patterns of MWCNTs and OMWCNTs

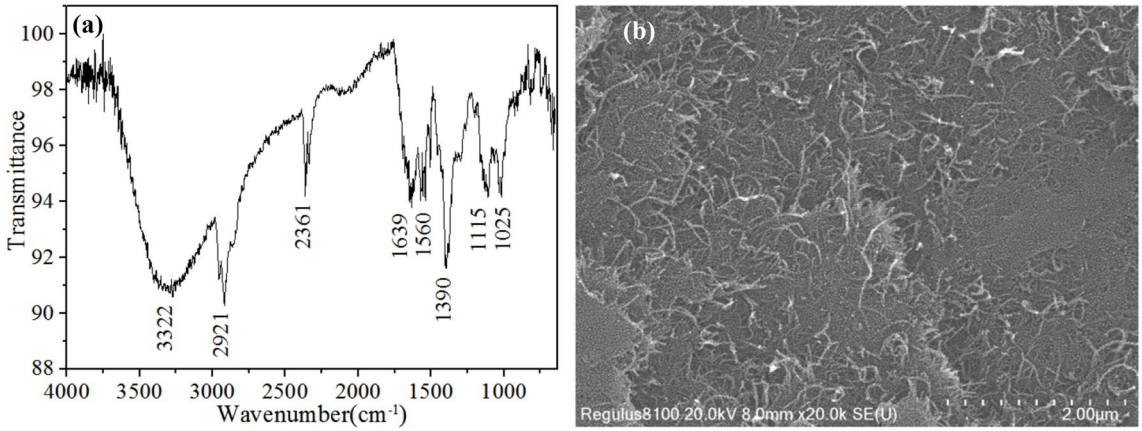

Fig. 2 **a** FT-IR spectrum and **b** SEM image of OMWCNTs

groups of carboxylic acids and alcohols [19]. The peak at 2361 cm^{-1} is associated with the O–H stretching of carboxylic acids [20]. The peaks at 1639 and 1560 cm^{-1} are related to the vibration of C=O bond originating from carboxyl [20, 21]. The peak at 1390 cm^{-1} belongs to the stretching vibration of C–OH. The peak at 1115 cm^{-1} is related to the vibration of C–O bond originating from carboxyl [21]. The peak at 1025 cm^{-1} is attributed to the stretching vibration of C–O. Therefore, there are many carboxyl, carbonyl, and hydroxyl groups on the surface of OMWCNT treated by the mixed acid.

The morphological characteristic of OMWCNTs was investigated using SEM. Figure 2 shows the SEM image of OMWCNTs. It can be seen from the figure, the entangled network was observed for sample OMWCNTs.

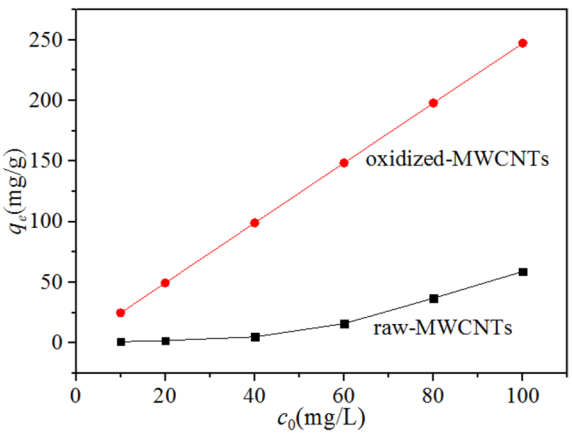

Fig. 3 Adsorption capacity of Pb(II) on MWCNTs and OMWCNTs

Influence of MWCNTs modification on adsorption properties

Many oxyen-containing functional groups of –OH and –COOH are produced after MWCNTs are oxidized by mixed acid, and these groups could well combine with Pb(II) in solution. In order to determine the important of –OH and –COOH groups generated by the oxidation treatment of MWCNTs in the adsorption and removal of Pb(II) from water. The adsorption capacity of Pb(II) on MWCNTs and OMWCNTs were investigated, as shown in Fig. 3. As can be seen from the figure, the adsorption capacity of Pb(II) on OMWCNTs is higher than that of Pb(II) on MWCNTs. The results illustrate that OMWCNTs have a larger adsorption capacity of Pb(II) than MWCNTs, and the –OH and –COOH groups of OMWCNTs participate in the adsorption of Pb(II) from water. In addition, as the initial concentration of Pb(II) increasing from 10 to 100 mg/L, the adsorption capacity of Pb(II) is also increased from 23.13 to 247.45 mg/g. This could be attributed to the increased concentration of Pb(II) migrating to the adsorbent surface.

Influence of contact time

Figure 4 shows the influence of contact time on the adsorption capacity of Pb(II) with different concentrations on OMWCNTs. As shown in the figure, the adsorption capacity of Pb(II) on OMWCNTs increase rapidly with the increase of contact time at the first 5 min. The adsorption equilibrium is reached at 5 min for 20 mg/L Pb(II) and 10 min for 100 mg/L Pb(II). The results indicate that the adsorption rate of Pb(II) on OMWCNTs is very fast.

Influence of OMWCNTs dosage

The batch adsorption experiments were carried out by using different amounts (10–35 mg) of OMWCNTs to study the

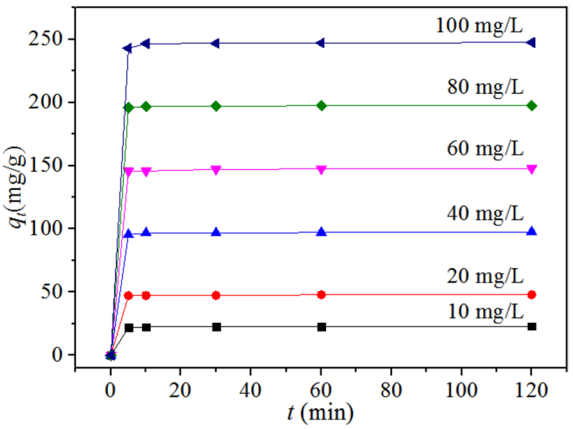

Fig. 4 Effect of contact time on adsorption capacity

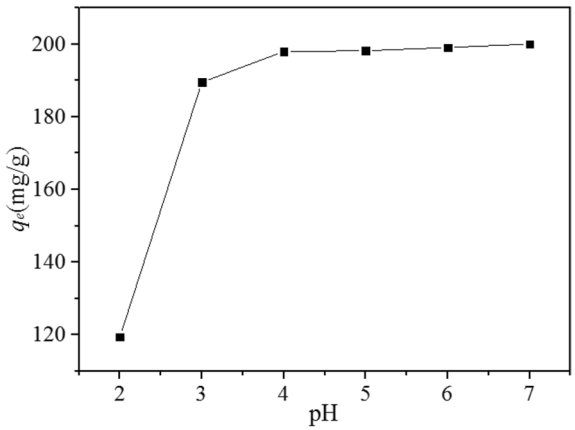

Fig. 6 Effect of pH on adsorption capacity

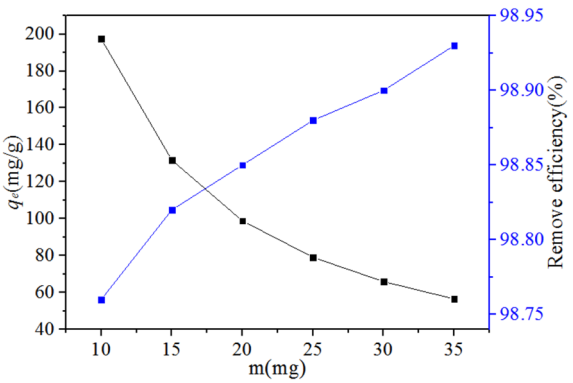

Fig. 5 Effect of OMWCNTs dosage on adsorption capacity and removal efficiency

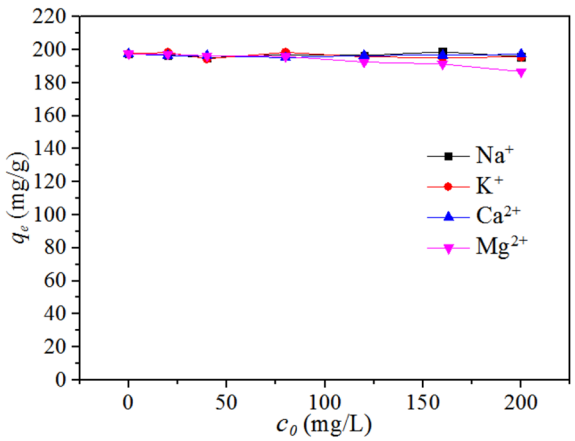

Fig. 7 Effect of coexisting ions (Na^+, K^+, Ca^{2+}, Mg^{2+}) on adsorption capacity

effect of adsorbent dosage on adsorption of Pb(II). As shown in Fig. 5, the adsorption capacity of Pb(II) decrease significantly with the increase of the amount of OMWCNTs. The removal efficiency of Pb(II) increase with the increase of OMWCNTs dosage, but the removal efficiency remained above 98.8%. Therefore, a small amount of OMWCNTs can achieve excellent adsorption and removal effect.

Effect of pH

pH can affect the adsorption effect by affecting the charge transfer at the solid–liquid interface. Therefore, the pH of solution could affect the adsorption of Pb(II) at a certain extent. Figure 6 shows the influence of pH on the adsorption of Pb(II) by OMWCNTs. It can be seen from the figure that, the adsorption capacity of Pb(II) on OMWCNTs increases with the increase of pH value in the range of pH = 2–5. The adsorption capacity of Pb(II) is stable when the pH = 5–7. This phenomenon can be explained by the zero charge point (PZC) of OMWCNTs. According to the literature [19], the PZC value of OMWCNTs is about 5. When the pH < 5, the surface of OMWCNTs is positively charged, which is not conducive to the adsorption of positively charged Pb(II) by OMWCNTs. When the pH value increased from 2 to 5, the positive charge on the surface of OMWCNTs decreased and the adsorption capacity of Pb(II) on OMWCNTs increased. When the pH > 5, the surface of OMWCNTs is negatively charged, which is conducive to the adsorption of Pb(II).

Influence of coexisting ions

Na^+, K^+, Ca^{2+}, Mg^{2+} are common ions in water. They may compete with Pb(II) adsorption on the surface of OMWCNTs and affect the adsorption of Pb(II) on OMWCNTs. In order to investigate the influence of co-existing ions (Na^+, K^+, Ca^{2+}, Mg^{2+}) on the adsorption of Pb(II) by MWCNTs, $NaNO_3$, KNO_3, $Ca(NO_3)_2$, and $Mg(NO_3)_2$ were used as ion sources for Pb(II) adsorption interference

experiments. The influence of co-existing ions on the adsorption capacity of Pb(II) is shown in Fig. 7. As can be seen from the figure, the adsorption capacity of Pb(II) is basically unchanged with the increase of concentration of coexisting ion. Therefore, the presence of Na^+, K^+, Ca^{2+} and Mg^{2+} have little effect on the adsorption of Pb(II) on OMWCNTs. The OMWCNTs could be widely used in water treatment.

Adsorption isotherms

Langmuir and Freundlich isotherms are the most commonly used to describe the adsorption characteristics of adsorbents in wastewater treatment. In this paper, Langmuir and Freundlich isotherm models have been used to fit and analyze the experimental data [22, 23].

Langmuir isothermal equation, $$\frac{C_e}{q_e} = \frac{1}{k_L q_L} + \frac{C_e}{q_L}$$

Freundlich isothermal equation, $$\ln q_e = \ln k_F + \frac{1}{n_F} \ln c_e$$

where c_e (mg/L) is the concentration of Pb(II) when the adsorption reached equilibrium; q_e (mg/g) is the adsorption capacity of Pb(II) on OMWCNTs when the adsorption reached equilibrium; q_L (mg/g) is the theoretical maximum adsorption capacity of Pb(II) on OMWCNTs; k_L is Langmuir constant; k_F and n_F are Freundlich constants.

The fitting results of Langmuir and Freundlich isothermal models for experimental data are shown in Fig. 8, and the fitting parameters are listed in Table 1. As can be seen from Table 1, Langmuir and Freundlich isothermal models are good agreement with experimental data, and correlation coefficients R^2 are 0.9789 and 0.9968, respectively. The good correlation coefficient of Langmuir and Freundlich isotherm models demonstrate that Pb(II) is adsorbed well on the surface of OMWCNTs. Thus, it is further illustrated that OMWCNTs have great potential in the removal of Pb(II) from wastewater.

Table 1 Isotherm parameters for Pb(II) adsorption on OMWCNTs

Langmuir isotherm			Freundlich isotherm		
q_L	k_L	R^2	n_F	k_F	R^2
558.66	0.5474	0.9789	1.2344	196.9205	0.9968

Adsorption kinetics

Adsorption kinetics is an important aspect of adsorption mechanism research. In this paper, the experimental data of adsorption of Pb(II) by OMWCNTs are fitted with Pseudo-first-order kinetic model, Pseudo-second-order kinetic model, Intraparticle diffusion and Elovich kinetic models [24–27].

Pseudo - first - order $$\ln(q_e - q_t) = \ln q_e - k_1 t$$

Pseudo - second - order $$t/q_t = 1/k_2 q_e^2 + t/q_e$$

Intraparticle diffusion $$q_t = k_{id} \cdot t^{0.5} + C$$

Elovich $$q_t = (1/\beta) \ln(\alpha \cdot \beta) + (1/\beta) \ln t$$

where k_1 (min^{-1}) and k_2 (g/mg min) are the Pseudo-first-order and Pseudo-second-order kinetic rate constant, respectively. k_{id} (mg g^{-1} $min^{-1/2}$) is the Intraparticle diffusion rate constant. α (mmol g^{-1} min^{-1}) is the Elovich initial adsorption rate, β (g $mmol^{-1}$) is the Elovich desorption constant.

The kinetic fitting results are shown in Fig. 9, and the fitting constants are listed in Table 2. Compared to the other

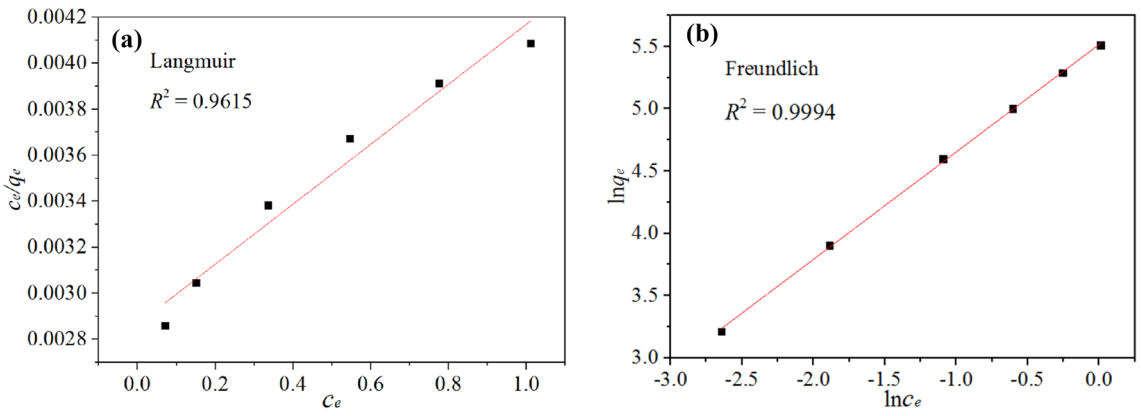

Fig. 8 **a** Langmuir and **b** Freundlich isotherm for Pb(II) adsorption on OMWCNTs

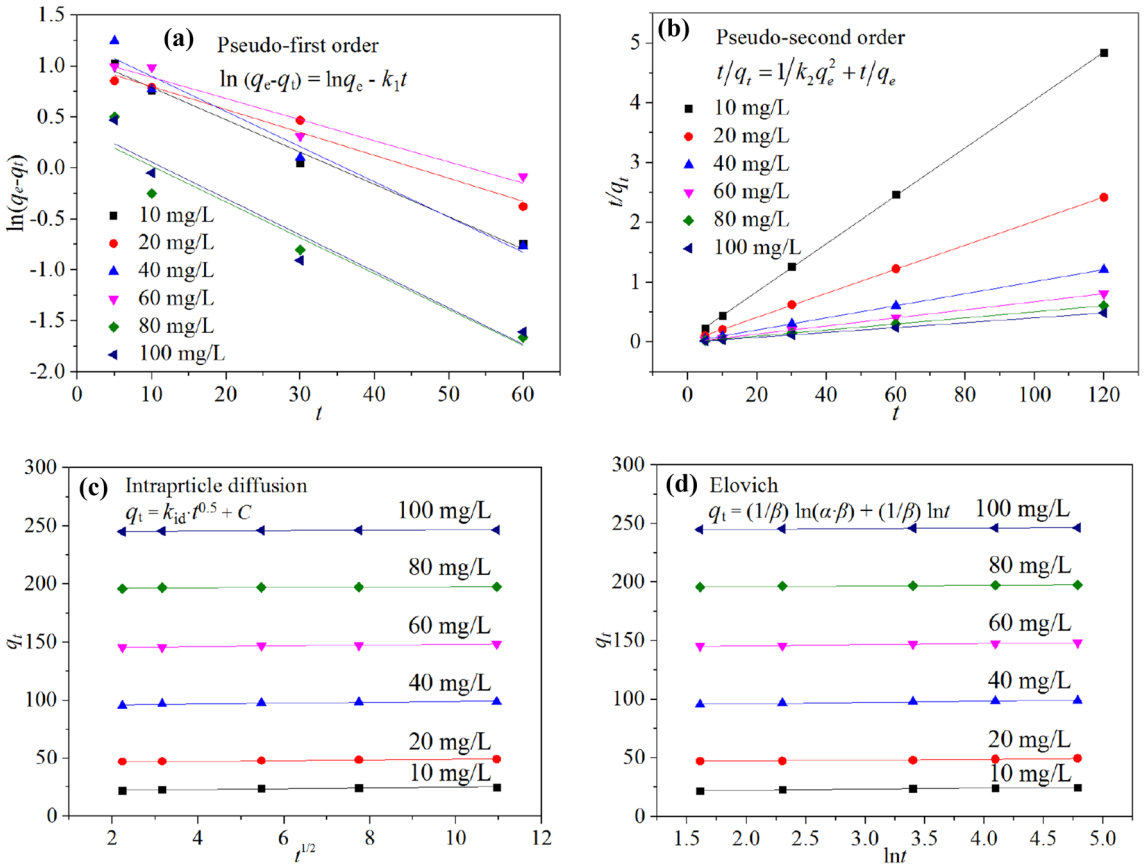

Fig. 9 Fitting curve of **a** Pseudo-first-order, **b** Pseudo-second-order, **c** Intraparticle diffusion and **d** Elovich kinetic model

Table 2 Kinetic parameters for Pb(II) adsorption on OMWCNTs

Kinetic model	Parameter	Value					
		10	20	40	60	80	100
Pseudo-first-order	k_1 (mg min g^{-1})	0.0317	0.0225	0.03454	0.02076	0.03517	0.03578
	q_e (mg g^{-1})	3.02545	2.78476	3.47554	2.99672	1.447807	1.51637
	R^2	0.98287	0.96877	0.95974	0.92777	0.88702	0.91568
Pseudo-second-order	k_2 (mg min g^{-1})	0.03536	0.03059	0.03511	0.02931	0.087402	0.08566
	q_e (mg g^{-1})	24.9626	49.7265	99.1080	148.368	197.6285	246.305
	R^2	0.9999	0.99991	0.99999	0.99999	1.0	1.0
Intraparticle diffusion	k_{id} (mg g^{-1} $min^{-1/2}$)	0.31599	0.28301	0.36762	0.32463	0.16138	0.16625
	R^2	0.89774	0.98415	0.81947	0.95735	0.69259	0.76567
Elovich	α (mmol g^{-1} min^{-1})	8.2×10^{9}	1.5×10^{26}	2.5×10^{38}	4.5×10^{70}	3.8×10^{177}	1×10^{217}
	β (g $mmol^{-1}$)	1.11403	1.32401	0.93909	1.13149	2.096744	2.04956
	R^2	0.99412	0.92052	0.95909	0.9449	0.8639	0.93154

three models, the pseudo-second-order kinetic model fitted well with the experimental data ($R^2 = 0.9999$), which indicating that the adsorption rate is mainly depended on the chemisorption process. Chemical reactions contribute greatly to the adsorption rate. This is consistent with the previous results that -OH and -COOH contribute greatly to the adsorption of Pb(II).

XPS investigation

In order to investigate the adsorption mechanism of Pb(II) on OMWCNTs, OMWCNTs were characterized by XPS before and after adsorption of Pb(II). XPS wide-scan spectra of OMWCNTs before and after adsorption of Pb(II) are shown in Fig. 10a. As shown in the figure, there are Pb 4f 7/2 and Pb 4f 5/2 peaks in the OMWCNTs after adsorption of Pb(II), indicating that Pb(II) is indeed adsorbent on the OMWCNTs. Figure 10b shows the C 1s high resolution XPS spectra of OMWCNTs before and after adsorption of Pb(II). The peak of typical graphite carbon at 284.7 eV represents the C 1s binding energy of OMWCNTs [28]. There is no significant difference in the C 1s spectra of the two samples, indicating that there is no significant influence on C of OMWCNTs before and after adsorption of Pb(II). Figure 10c shows the O 1s high resolution XPS spectra of OMWCNTs before and after adsorption of Pb(II). The experimental data showed that there are functional groups on the surface of OMWCNTs: carboxyl oxygen [O–C=O(H), 533.6 eV] and carbonyl oxygen [=C=O, 530.7 eV] [29]. As shown in Fig. 10c, there are significant differences in oxygen peaks of OMWCNTs before and after adsorption of Pb(II). The adsorption of Pb(II) was accompanied by the change of O binding energy, which suggesting that O-functional groups on the surface of OMWCNTs participated in the adsorption of Pb(II). As can be seen from Fig. 10d, after adsorption of Pb(II), the binding energies of Pb 4f 7/2 and Pb 4f 5/2 were 139.2 and 144.1 eV. Compared to the XPS spectra of pure $Pb(NO_3)_2$ reported in the literature [30], the characteristic peaks of Pb 4f 7/2 and Pb 4f 5/2 of pure $Pb(NO_3)_2$ were located at 139.6 and 144.5 eV, respectively. Obviously, after adsorption of Pb(II) on OMWCNTs, the characteristic peaks of Pb 4f 7/2

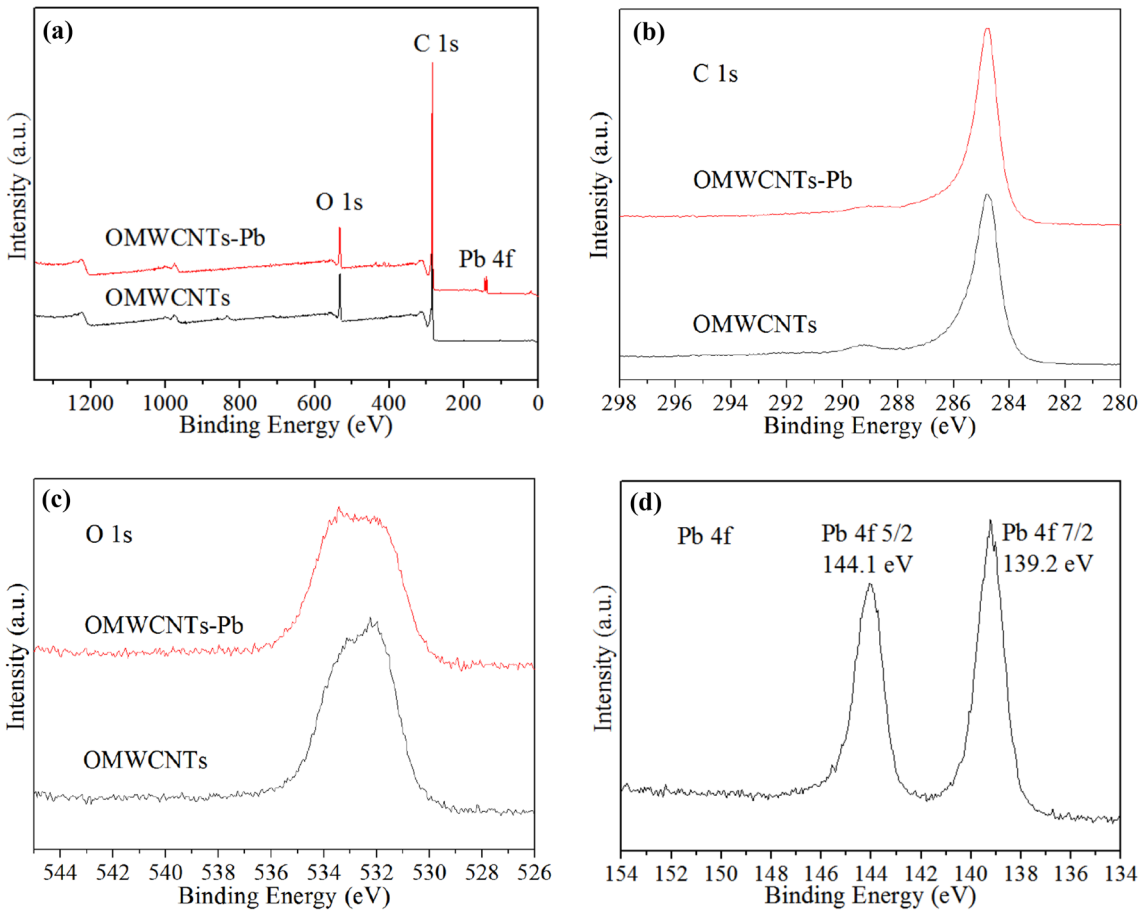

Fig. 10 XPS wide-scan (**a**), C 1s (**b**) O 1s (**c**) spectra of OMWCNTs before and after Pb(II) adsorption, **d** Pb 4f XPS spectra of OMWCNTs after Pb(II) adsorption

and Pb 4f 5/2 shifted to low values, respectively. The existence of affinity between OMWCNTs and Pb(II) was further proved by the shift of 0.4 eV.

Conclusions

In this paper, the adsorption of Pb(II) from water by MWCNTs and OMWCNTs were compared. Characterization analysis of OMWCNTs showed that –OH and –COOH were successfully modified on the MWCNTs. Compared to MWCNTs, OMWCNTs exhibit excellent adsorption capacity for Pb(II). The adsorption of Pb(II) by OMWCNTs was influenced significantly by pH. When pH < 5, the adsorption capacity increases obviously with the increase of pH value. When pH > 5, adsorption capacity is stable. The removal efficiency of Pb(II) by OMWCNTs was above 98.8%. The co-existing ions (Na^+, K^+, Ca^{2+} and Mg^{2+}) have little effect on the adsorption of Pb(II) by OMWCNTs. Adsorption isotherms can be well described by Freundlich and Langmuir model. The adsorption process accords with the pseudo-second-order kinetic model. Therefore, OMWCNTs is a potential adsorbent for removing Pb(II), and it has a good application prospect in removing Pb(II) from water.

Acknowledgements This project was supported by National Key Research and Development Program of China (2016YFC0400708), The Funding of Guizhou Provincial Department of Science & Technology ([2017]5409, [2020]6001), The Special Funding of Guiyang Science and Technology Bureau and Guiyang University (GYU-KY-[2022]), Innovation Group Project of Guizhou Provincial Department of Education (2020024).

References

1. S.B. Yang, C.L. Chen, Y. Chen, J.X. Li, D.Q. Wang, X.K. Wang, W.P. Hu, ChemPlusChem **80**, 480–484 (2015)
2. D. Wu, Y.G. Wang, Y. Li, Q. Wei, L.H. Hu, T. Yan, R. Feng, L.G. Yan, B. Du, J. Mol. Liq. **277**, 181–188 (2019)
3. P. Sharma, A.K. Singh, V.K. Shahi, ACS Sustain. Chem. Eng. **7**, 1427–1436 (2019)
4. M. Mohammadyan, M. Moosazadeh, A. Borji, N. Khanjani, S.R. Moghadam, Environ. Monit. Assess. **191**, 126 (2019)
5. J.Y. Wang, Y.C. Li, Z.M. Lv, Y. Xie, J.J. Shu, A. Alsaedi, T. Hayat, C.L. Chen, J. Colloid Interface Sci. **542**, 410–420 (2019)
6. W. Xu, Y. Song, K. Dai, S. Sun, G. Liu, J. Yao, J. Hazard. Mater. **358**, 337–345 (2018)
7. R. Mehrkhah, E.K. Goharshadi, M.M. Ghafurian, M. Mohammadi, O. Mahian, Sol. Energy **224**, 440–454 (2021)
8. R. Mehrkhah, E.K. Goharshadi, M. Mohammadi, J. Ind. Eng. Chem. **101**, 334–347 (2021)
9. M. Karimi-Nazarabad, E.K. Goharshadi, R. Mehrkhah, M. Davardoostmanesh, Sep. Purif. Technol. **279**, 119788 (2021)
10. M. Karimi, M.H. Entezari, M. Chamsaz, Ultrason. Sonochem. **17**, 711–717 (2010)
11. T. Amini, P. Hashemi, A. Kakanejadifard, J. Iran. Chem. Soc. **17**, 1967–1976 (2020)
12. M. Karimi-Nazarabad, H. Azizi-Toupkanloo, J. Iran. Chem. Soc. (2021). https://doi.org/10.1007/s13738-021-02398-3
13. H. Zhao, X. Liu, Z. Cao, Y. Zhan, X.D. Shi, Y. Yang, J.L. Zhou, J. Xu, J. Hazard. Mater. **310**, 235–245 (2016)
14. B. Shrestha, T.A. Anderson, V. Acosta-Martinez, P. Payton, J.E. Cañas-Carrell, Ecotox. Environ. Safety **116**, 143–149 (2015)
15. W.L. Sun, B.F. Jiang, F. Wang, N. Xu, Chem. Eng. J. **264**, 645–653 (2015)
16. ŞS. Bayazit, İ İnci, J. Ind. Eng. Chem. **19**, 2064–2071 (2013)
17. A.A. Farghali, H.A.A. Tawab, S.A.A. Moaty, R. Khaled, J. Nanostruct. Chem. **7**, 101–111 (2017)
18. L. Jiang, S. Li, H. Yu, Z. Zou, X. Hou, F. Shen, C. Li, X. Yao, Appl. Surf. Sci. **369**, 398–413 (2016)
19. N.D.V. Quyen, T.N. Tuyen, D.Q. Khieu, V.M.H. Ho, D.X. Tin, P.T.N. Lan, I. Kiyoshi, Bull. Mater. Sci. **41**, 6 (2018)
20. M.A. Atieh, O.Y. Bakather, B. Al-Tawbini, A.A. Bukhari, M.B. Fettouhi, Bioinorg. Chem. Appl. **11**, 603978 (2010)
21. Y.G. Wang, L.H. Hu, G.Y. Zhang, T. Yan, L.G. Yan, Q. Wei, B. Du, J. Colloid Interface Sci. **494**, 380–388 (2017)
22. Q.P. Fu, J. Lou, R.B. Zhang, L. Peng, S.Q. Zhou, W. Yan, C.L. Mo, J. Luo, J. Solid State Chem. **294**, 121836 (2021)
23. C.O. Chong, J. Rajan, S.M.S. Mohamed, Chem. Eng. J. **388**, 124306 (2020)
24. E.K. Goharshadi, M.B. Moghaddam, Int. J. Environ. Sci. Technol. **12**, 2153–2160 (2015)
25. B. Tural, E. Ertaş, M. Güzel, S. Tural, Appl. Water Sci. **11**, 128 (2021)
26. R.E. Alsohaimi, I.H. Alsohaimi, F.M. Mohamed, R.E. Khalifa, Cellulose **28**, 7165–7183 (2021)
27. Q.P. Fu, J. Lou, L. Peng, R.B. Zhang, S.Q. Zhou, P. Wu, W. Yan, C.L. Mo, J. Luo, J. Solid State Chem. **300**, 122188 (2021)
28. D. Xu, X.L. Tan, C.L. Chen, X.K. Wang, J. Hazard. Mater. **154**, 407–416 (2008)
29. A.M. Bond, W. Miao, C.L. Raston, Langmuir **16**, 6004–6012 (2000)
30. H.W. Hou, C.X. Yu, X. Han, Z.C. Shao, L.L. Liu, Cryst. Growth Des. **18**, 1474–1482 (2018)